



## Article

# Dielectric Stability of Triton X-100-Based Tissue-Mimicking Materials for Microwave Imaging

Mariana Relva<sup>1</sup> and Susana Devesa<sup>1,2,\*</sup>

<sup>1</sup> Instituto Politécnico de Coimbra, Coimbra Institute of Engineering, Department of Physics and Mathematics, Rua Pedro Nunes, Quinta da Nora, 3030-199 Coimbra, Portugal; mariana.relva10@gmail.com

<sup>2</sup> CEMMPRE, Centre for Mechanical Engineering, Materials and Processes, Department of Mechanical Engineering, University of Coimbra, Rua Luís Reis Santos, 3030-788 Coimbra, Portugal

\* Correspondence: susanamdevesa@ua.pt

**Abstract:** Microwave imaging is an emerging technology, and has been proposed for various applications, namely as an alternative diagnostic technology. Microwave imaging explores the dielectric contrast of target tissues, enabling diagnosis based on the differences in dielectric properties between healthy and diseased tissues, with low cost, portability and non-ionizing radiation as its main advantages, constituting an alternative to various imaging technologies for diagnosing and monitoring. Before clinical trials of microwave imaging devices for the study of dielectric properties, phantoms are used, mimicking the materials of tissues and simulating the electric properties of human tissues, for device validation. The purpose of this work was to prepare and perform dielectric characterization of mimicking materials for the development of an anthropomorphic phantom of the human ankle with realistic dielectric and anatomic properties. The biological tissues targeted in this investigation were the skin, muscle, cortical bone, trabecular bone and fat, with the mimicking materials prepared using Triton X-100, sodium chloride and distilled water. The dielectric characterization was performed using a coaxial probe, operating at frequencies between 0.5 and 4.0 GHz. Since the stability of the dielectric properties of mimicking materials is one of their main properties, the dielectric characterization was repeated after 15 and 35 days.

**Keywords:** mimicking materials; microwave imaging; dielectric properties; Triton X-100; coaxial probe



**Citation:** Relva, M.; Devesa, S. Dielectric Stability of Triton X-100-Based Tissue-Mimicking Materials for Microwave Imaging. *Spectrosc. J.* **2023**, *1*, 72–85. <https://doi.org/10.3390/spectroscj1020007>

Academic Editor: Clemens Burda

Received: 12 June 2023

Revised: 27 July 2023

Accepted: 31 July 2023

Published: 3 August 2023



**Copyright:** © 2023 by the authors. Licensee MDPI, Basel, Switzerland. This article is an open access article distributed under the terms and conditions of the Creative Commons Attribution (CC BY) license (<https://creativecommons.org/licenses/by/4.0/>).

## 1. Introduction

In recent years, the progress in microwave imaging technology has led to extensive studies for the development of tissue-mimicking materials that are dielectrically accurate, since the dielectric properties, specifically the dielectric constant and conductivity, of biological tissues characterize the interaction of electromagnetic waves with tissue [1,2].

Microwave imaging technology uses the dielectric contrast of the targeted tissues, enabling diagnosis based on the differences in the dielectric properties between healthy and unhealthy tissues, presenting as its main advantages low cost, portability and the non-ionizing nature of radiation, constituting an alternative to various imaging technologies used for diagnosis and monitoring [1,3–5].

Microwave imaging has made significant progress as a future alternative imaging technique for medical applications, particularly for breast cancer and cerebrovascular accident diagnosis, but it has also been proposed for in vivo measurement of the dielectric properties of the human calcaneus and wrist for osteoporosis monitoring, and of the tibia for fracture monitoring [1,4,6–8].

Before clinical trials on humans or animals, microwave imaging systems are tested on artificial phantoms that have the same anatomy and dielectric properties as human tissues. Therefore, tissue-mimicking materials are essential to the evaluation of the repeatability, stability, imaging quality and resolution of a microwave imaging system [1,2,5].

Over the years, numerous different tissue-mimicking materials have been created to mimic the properties of low-water-content and high-water-content biological tissues at discrete frequencies [9], mainly in the context of hyperthermia studies.

In 1971, Guy [10] developed a mixture composed of Laminac 4110, a polyester resin, acetylene black and aluminum powder to mimic fat and bone (low-water-content tissues) and a mixture of NaCl solution, powdered polyethylene and a gelling agent to mimic muscle (a high-water-content tissue), at a range of frequencies around 100–1000 MHz.

Cheung and Koopman [11], in 1976, studied these same materials, varying their composition, to mimic human tissues at two discrete frequencies, 8.5 and 10 GHz.

In 1984, Chou et al. [12], using the same materials proposed by Guy, and varying the relative amount of the components, performed dielectric characterization, at three different temperatures, at discrete frequencies between 13.56 and 2450 MHz. Despite their apparently promising results, the useful life of the developed phantoms was limited to two weeks. The inconvenience of the gelling agent, in this case, TX 150, having a variable setting time was mentioned by the authors.

In the same year, Bini et al. [13] tested another type of mixture that, in 1988, was also studied by Andreuccetti et al. [14], whose main component was polyacrylamide gel. These phantoms were attractive because of their optical transparency and gelatinous mechanical properties. However, their useful life was quite limited: when exposed to air, a few hours, and when kept in an airtight container, a few weeks. These works mimicked the dielectric characteristics of bone and fat, at 27 MHz and in a frequency range of 0.75–5.5 GHz, respectively [9,13,14].

In 1985, Lagendijk and Nilsson [15] developed phantoms that consisted of a mixture of flour, oil and saline solution, to model fat, whose dielectric properties were studied at a frequency of 451 MHz.

Marchal et al. [16], in 1989, described a phantom, consisting of water and gelatine, which simulated the dielectric characteristics of muscle tissue, at 10, 27 and 50 MHz. According to the authors, it was possible to keep the phantom in the open air for 2–4 weeks, albeit with the possibility of gradual dehydration and, consequently, alteration of its dielectric constant.

Other materials were tested in 1991 by Robinson et al. [17], who developed phantoms to simulate the dielectric properties of muscle and fat at 500, 1000 and 2450 MHz. The material that mimicked the muscle was composed of ethanediol, water, sodium chloride and gelatine, while ethanediol, gelatine, polyethylene powder and detergent were used to simulate fat.

In 1992, Surowiec et al. [18] proposed a polyacrylamide gel material that, at room temperature, proved to be effective in simulating muscle tissue, at 25 °C, at frequencies between 500 MHz and 3 GHz.

A material that uses silicone rubber with carbon fiber was described, in 1996, by Nikawa et al. [19]. By varying the relative proportion of two different types of carbon fibers, an extensive variety of dielectric constants and conductivities, measured in the range of 10 MHz to 10 GHz, were achieved, with the mimicry of different biological tissues being possible. In addition, and according to the authors, the absence of water made it possible to obtain phantoms that were stable over time and that did not require particular care in their conservation.

Chang et al. [20], in 2000, developed a solid conductive plastic that replicated the dielectric properties of muscle tissue at frequencies between 300 and 900 MHz. This phantom, composed of polyethyl methacrylate and black carbon, could be molded into any shape and presented dielectric properties that remain constant over time.

In 2002, Youngs et al. [21] developed a phantom, based on a conductive material dispersed in an insulating thermoplastic matrix, to mimic fat, muscle and grey matter. The dielectric characterization was performed between 1 MHz and 10 GHz.

Sunaga et al. [22], in 2003, described a phantom composed of gelatin, honey syrup, distilled water and sodium chloride, with the aim of simulating the dielectric properties of

human skin at four discrete frequencies between 64 and 400 MHz. The results obtained were promising; however, the stability of the dielectric properties of the phantom was only evaluated after one week.

In 2005, Lazebnik et al. [9] created a phantom that was characterized at frequencies from 500 MHz to 20 GHz, with the aim of reproducing the dielectric properties of various biological tissues. This material had a gelatinous base and contained different kerosene and safflower oil solutions, *n*-propanol, *p*-toluic acid, formaldehyde and a surfactant. According to the authors, an important feature of these materials was their capacity to create heterogeneous and anthropomorphic configurations with lasting stability in terms of their mechanical and electrical properties.

Pinto et al. [23], in 2014, described the use of gelatine as a phantom in electrical impedance spectroscopy measurements, performed from 100 kHz to 15 MHz. They used unflavored edible gelatine that was diluted in distilled water. Phantoms were also manufactured with different salt concentrations. In all solutions, formaldehyde was used to increase the melting temperature of the gelatine and its duration. In this study, the authors came to the conclusion that gelatine can be applied as a skin phantom in electrical impedance spectroscopy measurements.

Liquid mixtures based on Triton X-100, water and sodium chloride were adopted by Joachimowicz et al. [4] in 2017, Savazzi et al. [7] in 2020 and Amin et al. [1,24] in 2020 and 2021. In the first work mentioned [4], the authors mimicked the dielectric properties of cerebrospinal fluid, brain, blood, bone and muscle, in a frequency range from 0.5 to 6 GHz. Savazzi et al. [7] developed an anatomically and dielectrically accurate phantom of the axillary region, to be applied in experimental imaging evaluation of axillary lymph nodes using microwave imaging technology. Finally, Amin et al. [24] mimicked the dielectric properties of cortical bone, trabecular bone and skin, at frequencies between 0.5 and 8.5 GHz, to develop a three-dimensional phantom of the structure of the human heel.

Many of the described materials simulated, adequately, the dielectric properties of tissues, but only in the narrowband spectra for which they were designed. On the other hand, Triton X-100 has been described as an exceptional candidate for a liquid-based phantom. Mixtures based on Triton X-100 and sodium chloride solutions are able to simulate the dielectric properties of various human tissues in a large frequency range. The liquid nature of Triton X-100 solutions guarantees that complex three-dimensional structures can be filled while avoiding air bubbles. Another advantage of these mixtures is that their electromagnetic parameters can be predicted as a function of Triton X-100 and sodium chloride concentrations, using binary fluid mixture models such as Böttcher's formula. Finally, tissue-mimicking materials are easily produced and time-stable [1,4,5,7,24].

The interactions of electromagnetic radiation with matter can be quantified through complex relative permittivity,  $\epsilon^*$ , where the permittivity of the medium describes its tendency to be polarized when an electromagnetic field is applied:

$$\epsilon^* = \epsilon' - j\epsilon'' = \epsilon' - j\frac{\sigma}{\epsilon_0\omega} \quad (1)$$

where  $\epsilon'$  is the real part of the complex permittivity, generally known as the dielectric constant or relative permittivity, and is related to the ability of the material to store energy from the applied electric field;  $\epsilon''$  is the imaginary part of the complex permittivity, also identified as a loss factor, and reflects the dissipative nature of the material, converting it to heat a fraction of the absorbed energy; the conductivity,  $\sigma$ , is related to the imaginary part of the complex permittivity via the relationship expressed in Equation (1);  $\omega$  is the angular frequency and  $\epsilon_0$  is the permittivity of the vacuum [25–28].

There are several mathematical functions that have been proposed to model the dielectric performance of polar materials and biological tissues. With these models, it is possible to calculate the dielectric constant and conductivity values at a specific frequency range, for which the relaxation equation is suitable.

One of the most frequent models that have been applied to replicate the electrical behavior of organic tissues or aqueous electrolytic solutions is the Cole–Cole model:

$$\varepsilon^* = \varepsilon_\infty + \frac{\varepsilon_s - \varepsilon_\infty}{1 + (j\omega\tau)^{1-\alpha}} + \frac{\sigma_s}{j\omega\varepsilon_0} \quad (2)$$

where  $\varepsilon_\infty$  represents the permittivity at infinite frequencies due to electronic polarizability and  $\varepsilon_s$  the static (low-frequency) permittivity;  $\sigma_s$  represents the static conductivity, related to charge movements;  $\tau$  is the relaxation time of the material, which is the time taken for the molecules or dipoles to return to their original random orientation; and  $\alpha$  is an empirical variable that measures the broadening of the dispersion, the magnitude of which is described by  $\varepsilon_s - \varepsilon_\infty$  [5,26,28,29].

The real part of the permittivity,  $\varepsilon'$ , is given by [30]:

$$\varepsilon' = \varepsilon_\infty + (\varepsilon_s - \varepsilon_\infty) \frac{1 + (\omega\tau)^{1-\alpha} \sin\left(\frac{\alpha\pi}{2}\right)}{1 + 2(\omega\tau)^{1-\alpha} \sin\left(\frac{\alpha\pi}{2}\right) + (\omega\tau)^{2(1-\alpha)}} \quad (3)$$

and the conductivity by [16]:

$$\sigma = \varepsilon_0\omega \frac{(\varepsilon_s - \varepsilon_\infty)(\omega\tau)^{1-\alpha} \cos\left(\frac{\alpha\pi}{2}\right)}{1 + 2(\omega\tau)^{1-\alpha} \sin\left(\frac{\alpha\pi}{2}\right) + (\omega\tau)^{2(1-\alpha)}} \quad (4)$$

However, in Equation (2) is described a single relaxation, and biological tissues are generally described in terms of multiple Cole–Cole poles, where each pole of the equation describes the effect of a particular dispersion region. Therefore, if the dielectric behavior of a material is studied in a wide frequency range, the totality of the dielectric relaxations taking place over that frequency range must be considered, and more poles should be introduced to adequately describe the material. In this case, the Cole–Cole equation should be rewritten accordingly:

$$\varepsilon^* = \varepsilon_\infty + \sum_{n=1}^N \frac{\varepsilon_{s_n} - \varepsilon_\infty}{1 + (j\omega\tau_n)^{1-\alpha_n}} + \frac{\sigma_s}{j\omega\varepsilon_0} \quad (5)$$

where  $N$  is the number of fitting poles of the equation [5,27,29,30].

For the dielectric characterization of biological tissue, the 4-pole Cole–Cole model has been proposed [2,5,29].

The main goal of the work presented in this paper is the preparation, dielectric characterization and study of the dielectric property stability of the tissue-mimicking materials with relevance to human wrist and ankle anthropomorphic phantoms, aiming to enable the diagnosis and monitoring of bone diseases, like osteoporosis, in a non-invasive way, which can be achieved through a microwave imaging system.

Bone mineral density, usually measured via dual-energy X-ray absorptiometry, is considered a primary parameter in the diagnosis of osteoporosis. However, recent developments suggest a correlation between the dielectric properties of bone and its mineral density [3]. Amin et al. [3] presented results that suggest that the mean relative permittivity of the femoral head in a patient diagnosed with osteoarthritis is higher when compared to that in an osteoporotic patient. Ruchikerketta et al. [6] showed that as bone mineral density decreases with the beginning of osteoporosis, the dielectric constant and conductivity increase proportionately. Therefore, the study of bone dielectric properties is of supreme relevance for the development of microwave radiation-based medical devices for diagnosing osteoporosis or even assessing bone fracture risk [3,31].

The studied samples, composed of Triton X-100, deionized water and sodium chloride, were prepared to mimic the dielectric properties of skin, fat, muscle, cortical bone and trabecular bone.

The dielectric measurements were performed in a frequency range of 0.5–4.0 GHz, at room temperature, using the open-ended coaxial probe technique.

## 2. Materials and Methods

Several procedures are available in the literature to prepare liquid mimicking materials of human tissues [32]. For the present application, the target tissues were skin, fat, muscle, cortical bone and trabecular bone.

To simulate the dielectric properties of skin, fat, muscle, cortical bone and trabecular bone, several mixtures containing Triton X-100 (Rohm e Haas Co., Philadelphia, PA, USA), deionized water and sodium chloride (Pronalab) were prepared.

The composition of the tissue-mimicking materials was obtained from the following papers: fat—Bjelogrlic et al. [32] and Savazzi et al. [7]; muscle—Joachimowicz et al. [4]; skin, cortical bone and trabecular bone—Amin et al. [1].

The authors used Böttcher's model [4], given by Equation (6), to set the Triton X-100 and sodium chloride quantities required to produce the mixtures that mimic the various tissues by fitting the binary mixture equation to the Debye or Cole–Cole models.

$$\varepsilon_m = \varepsilon_1 + [3V_2\varepsilon_m(\varepsilon_2 - \varepsilon_1)/(2\varepsilon_m - \varepsilon_2)] \quad (6)$$

where the subscripts  $m$ , 1 and 2 stand for mixture, Triton X-100 and sodium chloride solution, respectively.

The composition of the prepared tissue-mimicking materials is presented in Table 1. For each composition, an aqueous solution of sodium chloride was prepared and added to the Triton X-100, according to the stipulated volume percentages. The obtained materials were stirred until homogeneity was achieved, and then, stored at room temperature and protected from light.

**Table 1.** Composition of the prepared tissue-mimicking materials.

Target Tissue	Triton X-100 (Volume %)	Deionized Water (Volume %)	NaCl (g/L)
Skin	40.0	60.0	5.200
Fat	100	0	0
Muscle	24.0	76.0	5.000
Cortical bone	77.0	23.0	0.800
Trabecular bone	69.5	30.5	0.800

The dielectric measurements were performed using an Agilent 85070E probe connected to an HP 8753D Network Analyzer, in a frequency range of 0.5–4.0 GHz.

Prior to the measurement, the system was calibrated using the open/short/deionized water, as a standard procedure [33].

The dielectric properties of the studied materials can be determined by inserting the probe into the sample, with no special fixtures or containers being required. The measurements are non-destructive and can be made in real time [34].

The open-ended coaxial probe was developed as a section of a straight rigid coaxial transmission line. One extremity was assembled as the input port, in the form of a coaxial connector, and the other extremity, after being cut off and machined as an open end, constituted the probe tip. The probe tip was inserted into the sample, and the electric field lines formed between the electrodes of the probe tip changed as they penetrated the material. Consequently, the reflected signal, in the form of the reflection coefficient  $R^*$ , could be measured at the probe input port using the Network Analyzer. This parameter is a complex quantity defined by its real and imaginary parts. Since  $R^*$  is a function of  $\varepsilon^*$ , and vice versa, the complex relative permittivity of the sample can be calculated from  $R^*$  through the software provided by the probe manufacturer and that comprise calculations based on the measurements previously performed during the probe calibration: open (without any sample—open end is in the air), short (open end is shorted by a conductive material) and a known liquid (deionized water in the present case) [35].

The conductivity of the sample was posteriorly calculated from the imaginary part of the complex relative permittivity using the relationship defined in Equation (1).

The schematic representation of the measurement setup is depicted in Figure 1.

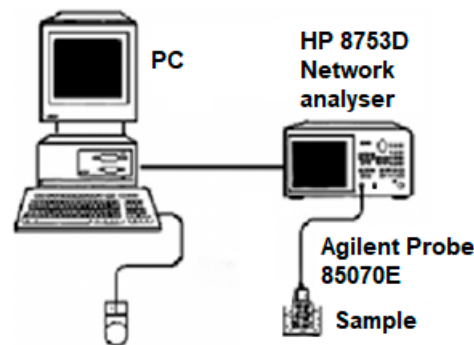


**Figure 1.** Experimental apparatus used for the measurement of the dielectric constant and dielectric losses (adapted from [36]).

Since the open-ended coaxial probe technique is very sensitive to Network Analyzer drifts and inappropriate handling of the probe [7], the calibration of the equipment was tested by measuring the dielectric properties of deionized water and comparing the experimental data with the values obtained using the Cole–Cole model, through Equations (3) and (4). The optimized parameters used were  $\epsilon_\infty = 4.22$ ,  $\epsilon_s = 79.9$ ,  $\tau = 8.8$  ps and  $\alpha = 0.013$  [34,37].

Figure 2 shows the dielectric constant and the conductivity (inset) of deionized water, measured at room temperature, and the data predicted by the Cole–Cole model.

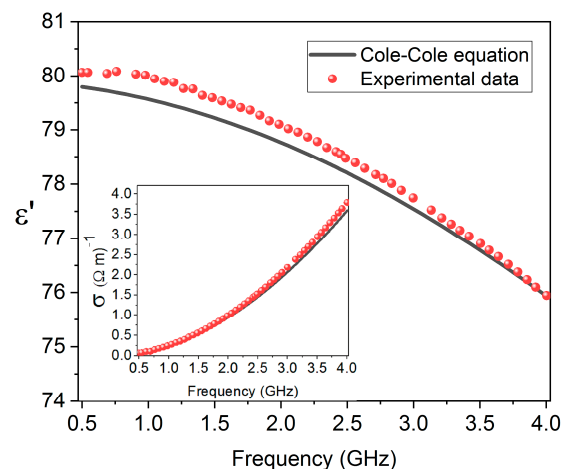


**Figure 2.** Frequency dependence of dielectric constant and conductivity (inset) of deionized water: measured values and those predicted by the Cole–Cole model.

The average percentage differences between the dielectric constant and conductivity of the measured values in relation to the data estimated by the Cole–Cole model were found to be 0.33% and 5.65%, respectively.

Besides the deionized water measurements and comparison with the Cole–Cole model, one of the tissue-mimicking materials was measured three times after the equipment calibration.

The maximum average percentage differences between the dielectric constant and conductivity of the measured values in relation to the mean value were 3.36% and 1.06%, respectively.

### 3. Results

The measured dielectric properties of the tissue-mimicking materials are shown in Figure 3. Besides the measured values, and for comparison, the values proposed by the IT'IS [38] database and calculated using the Cole–Cole model are also presented.

As previously mentioned, the four-pole Cole–Cole model was adopted, with the optimized parameters obtained from [15].

The dielectric parameters used in the IT'IS database are based on the Gabriel [39] dispersion relationships and, for that reason, in four of the five tissue-mimicking materials, the data from the database and estimated through the Cole–Cole model are very similar or even coincident, in the case of the dielectric constant values.

The dielectric constants of the tissue-mimicking materials are well aligned with the predicted values. Nevertheless, there is a significant deviation between the conductivity of fat- and cortical-bone-mimicking materials and the reference data.

In the case of cortical bone tissue mimicking, this mismatch occurs only at higher frequencies. The increase in the sodium chloride content could promote an increase in conductivity with a minor effect on the dielectric constant [40]; however, this adjustment would only benefit the high-frequency measurements, having a negative impact in the low-frequency zone. Moreover, the low-frequency band ranging from 0.5 to 2.4 GHz has more electromagnetic field penetration depth, which is reduced significantly above 3 GHz. Thus, this band is observed to be more feasible for microwave imaging applications [1].

Regarding the fat sample, composed only of Triton X-100, the experimental values are higher than the predicted ones, which means that the addition of sodium chloride is not the solution. However, other aspects must be taken under consideration, such as the higher viscosity of the samples with a higher percentage of Triton X-100, which can complicate the dielectric property measurements [40], or the fact that Böttcher's model does not work for every mixture [4].

Joachimowicz et al. [40] presented, for a fat-tissue-mimicking material, a percentage difference of 75%, with conductivity measured at 2.45 GHz, when compared to the Debye model, with the experimental value also being higher than the predicted one.

The average percentage differences between the experimental values and the reference data are presented in Table 2. As one can see, in all the samples, the experimental and reference data show better alignment for the dielectric constant. In the case of the fat- and cortical-bone-mimicking materials, the deviation from the experimental and reference values cannot be disregarded.

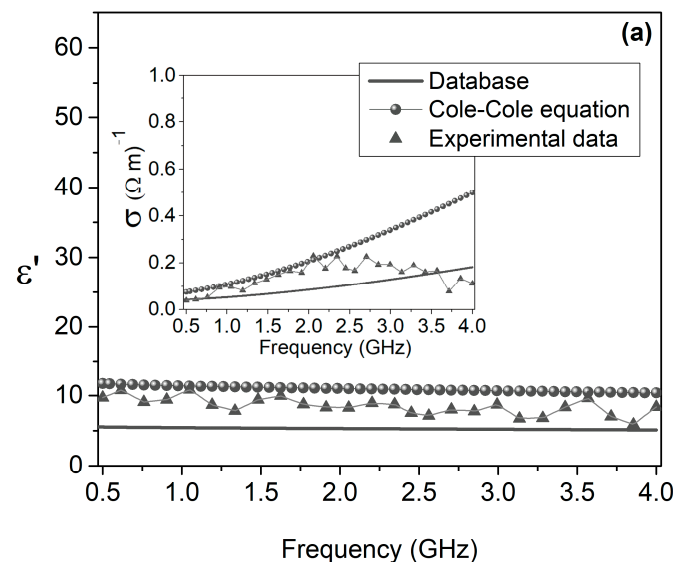


Figure 3. Cont.

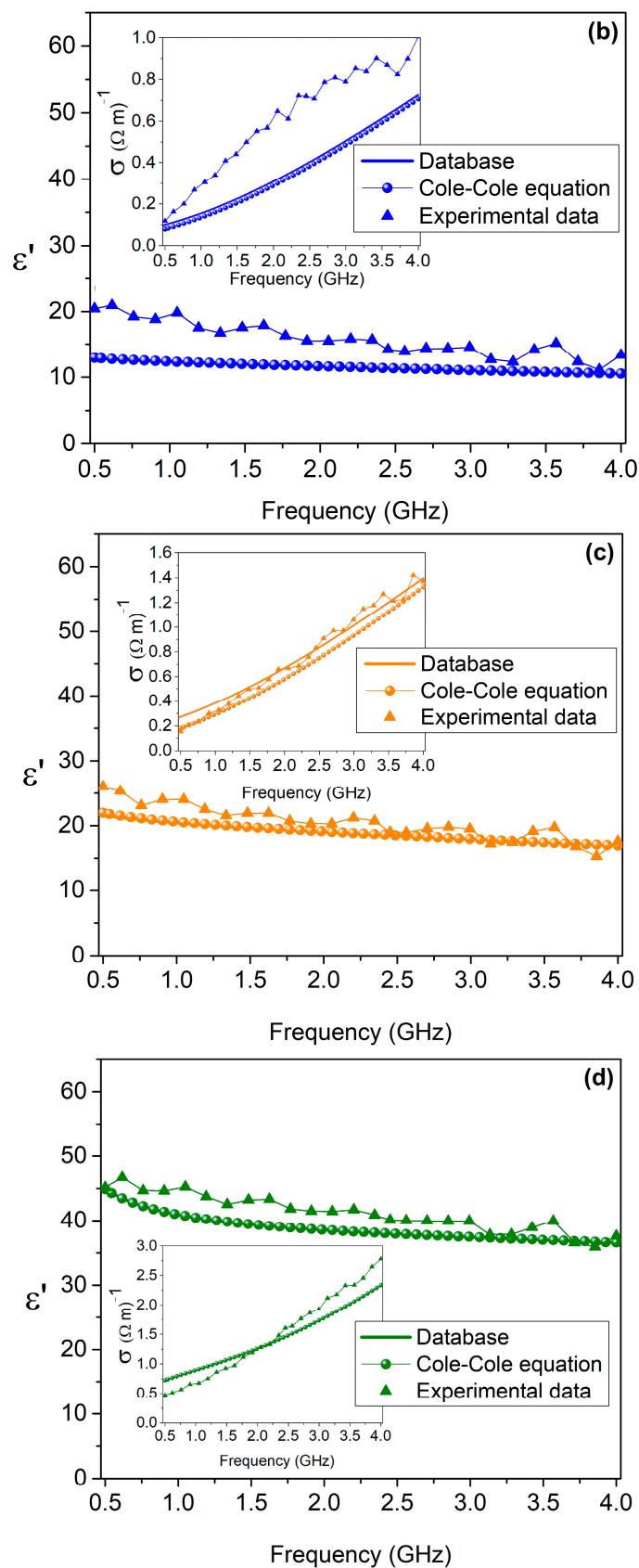
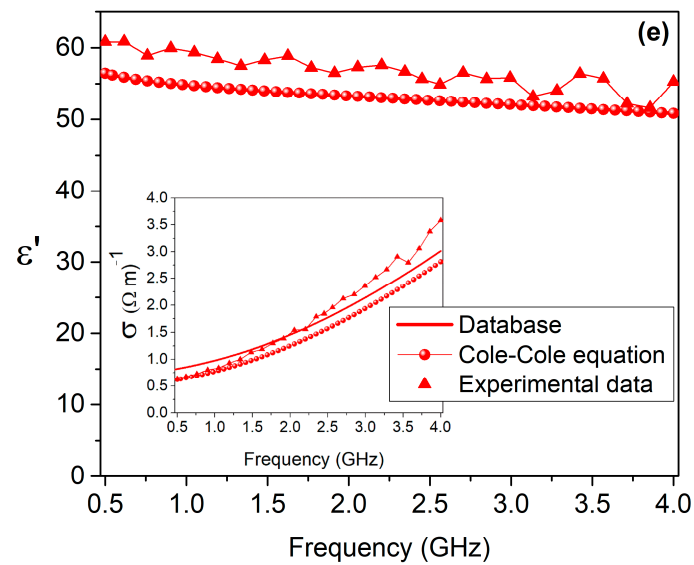


Figure 3. Cont.



**Figure 3.** Frequency dependence of dielectric constant and conductivity (inset) of the tissue-mimicking materials measured, predicted by the Cole–Cole model and proposed by the IT’IS database: (a) fat; (b) cortical bone; (c) trabecular bone; (d) skin; (e) muscle.

**Table 2.** Average percentage differences between the measured and the reference values proposed by the IT’IS database.

Tissue-Mimicking Material	Cole–Cole Model		IT’IS Database	
	$\Delta\epsilon'$ (%)	$\Delta\sigma$ (%)	$\Delta\epsilon'$ (%)	$\Delta\sigma$ (%)
Skin	6.09	15.17	6.20	14.77
Fat	22.83	30.43	58.14	62.65
Muscle	6.69	16.39	6.66	10.72
Cortical bone	35.34	83.56	34.88	70.46
Trabecular bone	8.98	11.84	9.21	8.62

To analyze the stability of the dielectric properties over time, they were measured three times, with a break of 15 days between the first and the second measurements and a break of 20 days between the second and third measurements.

Figure 4a, depicts the comparison between the three measured values of the dielectric constants. There does not exist a major difference between the values measured on the first two dates. Upon analyzing the third measurement, it is observed that there exist accentuated differences in the case of the muscle and the skin, with the dielectric constant showing lower values. In the cortical-bone-mimicking material, the dielectric constant stability is more accentuated.

Regarding the conductivity, presented in Figure 4b, it can be verified that there exists higher coherence between the values measured on the three dates.

Tables 3 and 4 show the dielectric constant and the conductivity, respectively, of the three measurements, at 2.45 GHz. Moreover, the percentage differences between the first and the second measurements, and between the first and the third measurements, are also presented.

These results are promising, since one of the fundamental characteristics of the mimicking materials is their stable dielectric properties over time, to guarantee the repeatability of the measurements.

To better understand the relationship between the composition of the tissue-mimicking materials and the stability of the dielectric properties over time, Figure 5a shows the percentage differences for the dielectric constant and conductivity as a function of the Triton X-100 percentage, and in Figure 5b, as a function of the NaCl content, for the first and third measurements, performed at 2.45 GHz. Both the dielectric constant and conductivity show the same trend, with the tissue mimicking the skin presenting the highest percentage differences.

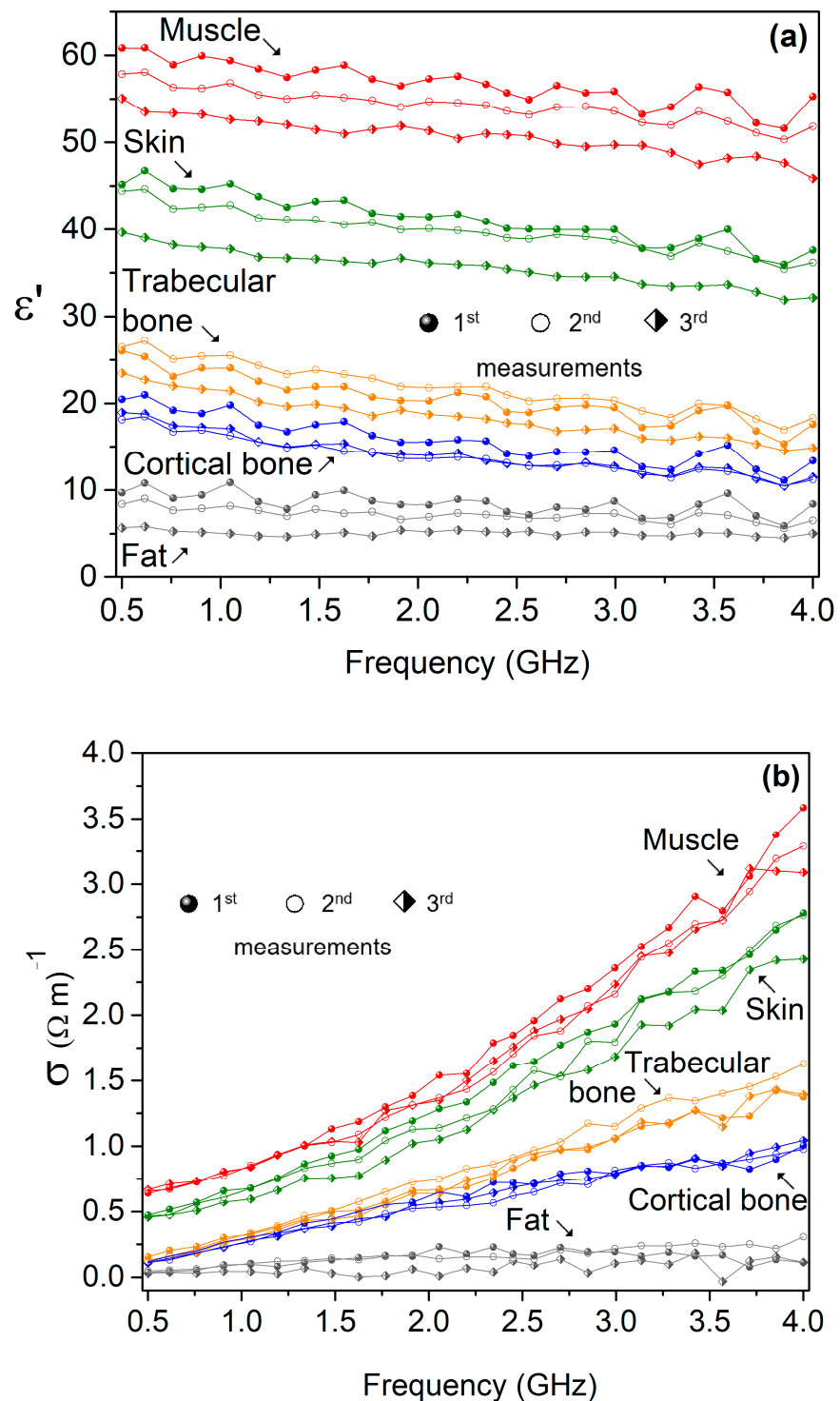


**Figure 4.** Frequency dependence of (a) dielectric constant and (b) conductivity of the tissue-mimicking materials, measured on different dates.

Since the high content of NaCl in the tissue mimicking the muscle did not compromise its dielectric stability, and the high percentage of Triton X-100 did not compromise the dielectric stability of the tissues mimicking the fat or the bone, it is valid to infer that the high content of NaCl, combined with the percentage of Triton X-100 of 40%, makes the preservation of the dielectric properties over time unfeasible.

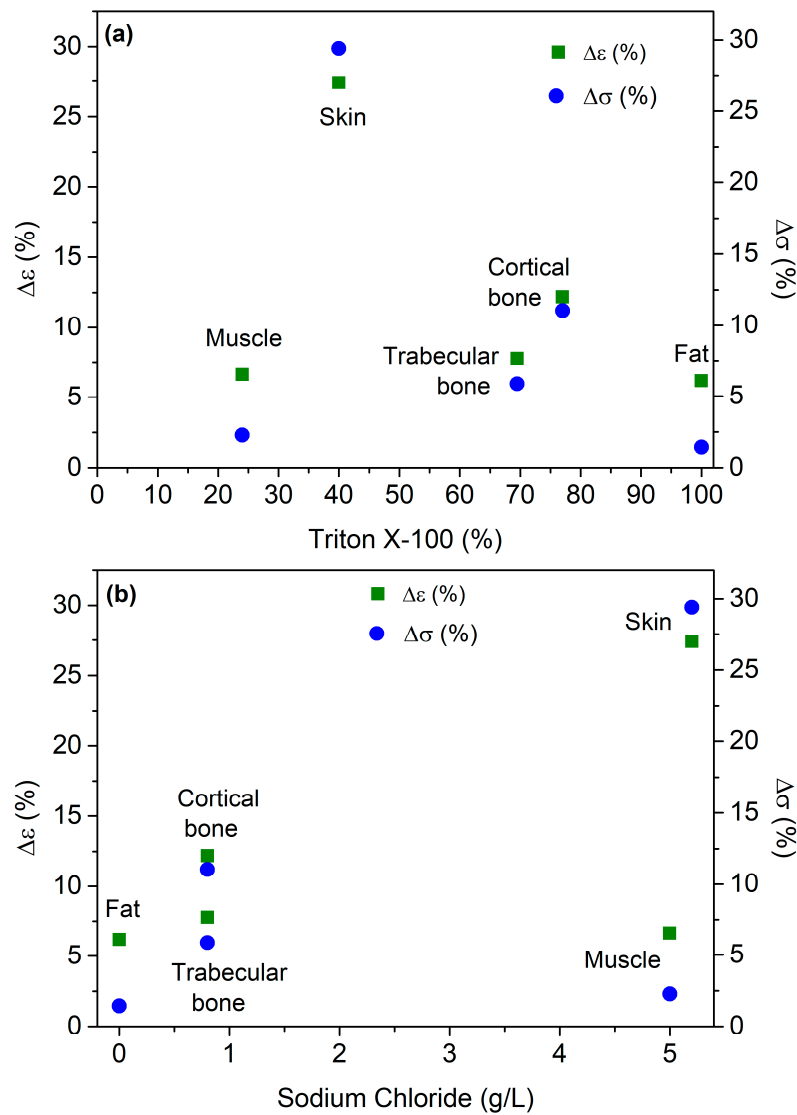


**Figure 5.** Dielectric constant and conductivity percentage differences between the first and third measurements, performed at 2.45 GHz, as a function of (a) Triton X-100 percentage and (b) sodium chloride content.

**Table 3.** Dielectric constant values, measured at 2.45 GHz, and respective percentage differences between the first and second measurements and the first and third measurements.

Tissue-Mimicking Material	Dielectric Constant, $\epsilon'$				
	1st Measurement	2nd Measurement	$\Delta\epsilon'$ (%)	3rd Measurement	$\Delta\epsilon'$ (%)
Skin	7.08	6.35	10.31	5.14	27.40
Fat	13.91	12.80	8.02	13.05	6.18
Muscle	19.01	20.21	6.29	17.75	6.63
Cortical bone	40.32	39.25	2.67	35.41	12.18
Trabecular bone	55.16	53.50	3.00	50.87	7.78

**Table 4.** Conductivity values, measured at 2.45 GHz, and respective percentage differences between the first and second measurements and the first and third measurements.

Tissue-Mimicking Material	Conductivity, $\sigma$				
	1st Measurement	2nd Measurement	$\Delta\sigma$ (%)	3rd Measurement	$\Delta\sigma$ (%)
Skin	0.17	0.13	23.99	0.12	29.41
Fat	0.70	0.66	6.88	0.69	1.43
Muscle	0.88	0.97	9.44	0.90	2.27
Cortical bone	1.54	1.52	1.07	1.37	11.04
Trabecular bone	1.87	1.78	4.57	1.76	5.88

#### 4. Conclusions

In this project, we successfully developed tissue-mimicking materials, based on Triton X-100, that replicate the dielectric properties of skin, muscle, fat, cortical bone and trabecular bone.

In the first phase, the permittivity and the dielectric losses of the samples, through which the conductivity was calculated, were measured and compared with the values available in the IT'IS database and computed using the Cole–Cole model.

The stability of the prepared samples was analyzed, whereby we measured their dielectric properties a second time (15 days later) and a third time (35 days later), revealing that for the samples mimicking fat, trabecular bone and cortical bone, promising results were achieved.

For the frequency of 2.45 GHz, considering the percentage differences between the original values obtained from the first measurements and the values measured 15 days later, it is possible to conclude that, of the five tissues studied, four of them, cortical bone, trabecular bone, skin and muscle, maintained their dielectric properties. Thirty-five days after the first measurement, dielectric stability was visible in the same four samples.

**Author Contributions:** Conceptualization, S.D.; methodology, S.D.; software, M.R. and S.D.; validation, S.D.; formal analysis, M.R. and S.D.; investigation, M.R. and S.D.; resources, S.D.; data curation, M.R. and S.D.; writing—original draft preparation, M.R. and S.D.; writing—review and editing, S.D.; visualization, S.D.; supervision, S.D.; project administration, S.D. All authors have read and agreed to the published version of the manuscript.

**Funding:** This research received no external funding.

**Institutional Review Board Statement:** Not applicable.

**Informed Consent Statement:** Not applicable.

**Data Availability Statement:** The raw/processed data required to reproduce these findings cannot be shared at this time, as the data also form part of an ongoing study.

**Acknowledgments:** The authors would like to thank the Laboratory of Electrical Measurements of the Physics Department of the University of Aveiro for the use of their Agilent 85070E probe.

**Conflicts of Interest:** The authors declare no conflict of interest.

#### References

1. Amin, B.; Kelly, D.; Shahzad, A.; O'Halloran, M.; Elahi, M.A. Anthropomorphic calcaneus phantom for microwave bone imaging applications. *IEEE J. Electromagn. RF Microw. Med. Biol.* **2021**, *5*, 206–213. [CrossRef]
2. Abedi, S.; Joachimowicz, N.; Meyer, O.; Picard, D.; Roussel, H. Phantoms for a novel generation of medical microwave imaging devices. In Proceedings of the 13th European Conference on Antennas and Propagation, Krakow, Poland, 31 March–5 April 2019; pp. 1–4.
3. Amin, B.; Elahi, M.A.; Shahzad, A.; Parle, E.; McNamara, L.; O'Halloran, M. An insight into bone dielectric properties variation: A foundation for electromagnetic medical devices. In Proceedings of the 1st World Conference on Biomedical Applications of Electromagnetic Fields, Split, Croatia, 10–13 September 2018; pp. 1–2. [CrossRef]

4. Joachimowicz, N.; Duchene, B.; Conessa, C.; Meyer, O. Reference phantoms for microwave imaging. In Proceedings of the 11th European Conference on Antennas and Propagation, Paris, France, 19–24 March 2017; pp. 2719–2722. [[CrossRef](#)]
5. Sultan, K.S.; Mohammed, B.; Mills, P.C.; Abbosh, A. Anthropomorphic durable realistic knee phantom for testing electromagnetic imaging systems. *IEEE J. Electromagn. RF Microw. Med. Biol.* **2020**, *5*, 132–138. [[CrossRef](#)]
6. Kerketta, S.R.; Ghosh, D. Microwave sensing for human bone health evaluation. *AEU-Int. J. Electron. Commun.* **2020**, *127*, 153469. [[CrossRef](#)]
7. Savazzi, M.; Abedi, S.; Ištuk, N.; Joachimowicz, N.; Roussel, H.; Porter, E.; O'Halloran, M.; Costa, J.R.; Fernandes, C.A.; Felício, J.M.; et al. Development of an anthropomorphic phantom of the axillary region for microwave imaging assessment. *Sensors* **2020**, *20*, 4968. [[CrossRef](#)]
8. Ramalingam, V.S.; Kanagasabai, M.; Sundarsingh, E.F. A Compact Microwave Device for Fracture Diagnosis of the Human Tibia. *IEEE Trans. Compon. Packag. Manuf. Technol.* **2019**, *9*, 661–668. [[CrossRef](#)]
9. Lazebnik, M.; Madsen, E.L.; Frank, G.R.; Hagness, S.C. Tissue-mimicking phantom materials for narrowband and ultrawideband microwave applications. *Phys. Med. Biol.* **2005**, *50*, 4245. [[CrossRef](#)]
10. Guy, A.W. Analyses of electromagnetic fields induced in biological tissues by thermographic studies on equivalent phantom models. *IEEE Trans. Microw. Theory Tech.* **1971**, *19*, 205–214. [[CrossRef](#)]
11. Cheung, A.Y.; Koopman, D.W. Experimental development of simulated biomaterials for dosimetry studies of hazardous microwave radiation. *IEEE Trans. Microw. Theory Tech.* **1976**, *24*, 669–673. [[CrossRef](#)]
12. Chou, C.K.; Chen, G.W.; Guy, A.W.; Luk, K.H. Formulas for preparing phantom muscle tissue at various radiofrequencies. *Bioelectromagnetics* **1984**, *5*, 435–441. [[CrossRef](#)]
13. Bini, M.G.; Ignesti, A.; Millanta, L.; Olmi, R.; Rubino, N.; Vanni, R. The polyacrylamide as a phantom material for electromagnetic hyperthermia studies. *IEEE Trans. Biomed. Eng.* **1984**, *3*, 317–322. [[CrossRef](#)]
14. Andreuccetti, D.; Bini, M.; Ignesti, A.; Olmi, R.; Rubino, N.; Vanni, R. Use of polyacrylamide as a tissue-equivalent material in the microwave range. *IEEE Trans. Biomed. Eng.* **1988**, *35*, 275–277. [[CrossRef](#)] [[PubMed](#)]
15. Lagendijk, J.J.W.; Nilsson, P. Hyperthermia dough: A fat and bone equivalent phantom to test microwave/radiofrequency hyperthermia heating systems. *Phys. Med. Biol.* **1985**, *30*, 709. [[CrossRef](#)]
16. Marchal, C.; Nadi, M.; Tosser, A.J.; Roussey, C.; Gaulard, M.L. Dielectric properties of gelatine phantoms used for simulations of biological tissues between 10 and 50 MHz. *Int. J. Hyperth.* **1989**, *5*, 725–732. [[CrossRef](#)]
17. Robinson, M.P.; Richardson, M.J.; Green, J.L.; Preece, A.W. New materials for dielectric simulation of tissues. *Phys. Med. Biol.* **1991**, *36*, 1565. [[CrossRef](#)]
18. Surowiec, A.; Shrivastava, P.N.; Astrahan, M.; Petrovich, Z. Utilization of a multilayer polyacrylamide phantom for evaluation of hyperthermia applicators. *Int. J. Hyperth.* **1992**, *8*, 795–807. [[CrossRef](#)]
19. Nikawa, Y.; Chino, M.; Kikuchi, K. Soft and dry phantom modeling material using silicone rubber with carbon fiber. *IEEE Trans. Microw. Theory Tech.* **1996**, *44*, 1949–1953. [[CrossRef](#)]
20. Chang, J.T.; Fanning, M.W.; Meaney, P.M.; Paulsen, K.D. A conductive plastic for simulating biological tissue at microwave frequencies. *IEEE Trans. Electromagn. Compat.* **2000**, *42*, 76–81. [[CrossRef](#)]
21. Youngs, I.J.; Treen, A.S.; Fixter, G.; Holden, S. Design of solid broadband human tissue simulant materials. *IEEE Sci. Meas. Technol.* **2002**, *149*, 323–328. [[CrossRef](#)]
22. Sunaga, T.; Ikehira, H.; Furukawa, S.; Tamura, M.; Yoshitome, E.; Obata, T.; Shinkai, H.; Tanada, S.; Murata, H.; Sasaki, Y. Development of a dielectric equivalent gel for better impedance matching for human skin. *Bioelectromagnetics* **2003**, *24*, 214–217. [[CrossRef](#)]
23. Pinto, A.M.; Bertemes-Filho, P.; Paterno, A.S. Caracterização de Gelatina como Fantoma para Medições de Espectroscopia de Impedância elétrica. In Proceedings of the XXIV Congresso Brasileiro de Engenharia Biomédica, Uberlândia, Brazil, 13–17 October 2014; pp. 1317–1320. [[CrossRef](#)]
24. Amin, B.; Kelly, D.; Shahzad, A.; O'Halloran, M.; Elahi, M.A. Microwave calcaneus phantom for bone imaging applications. In Proceedings of the 14th European Conference on Antennas and Propagation (EuCAP), Copenhagen, Denmark, 15–20 March 2020; pp. 1–5. [[CrossRef](#)]
25. Devesa, S.; Graça, M.P.; Henry, F.; Costa, L.C. Microwave dielectric properties of  $(\text{Bi}_{1-x}\text{Fe}_x)\text{NbO}_4$  ceramics prepared by the sol-gel method. *Ceram. Int.* **2015**, *41*, 8186–8190. [[CrossRef](#)]
26. Fornes-Leal, A.; Cardona, N.; Frasson, M.; Castelló-Palacios, S.; Nevárez, A.; Beltrán, V.P.; Garcia-Pardo, C. Dielectric characterization of in vivo abdominal and thoracic tissues in the 0.5–26.5 GHz frequency band for wireless body area networks. *IEEE Access* **2019**, *7*, 31854–31864. [[CrossRef](#)]
27. Sun, J.; Wang, W.; Yue, Q. Review on microwave-matter interaction fundamentals and efficient microwave-associated heating strategies. *Materials* **2016**, *9*, 231. [[CrossRef](#)]
28. La Gioia, A.; Porter, E.; Merunka, I.; Shahzad, A.; Salahuddin, S.; Jones, M.; O'Halloran, M. Open-ended coaxial probe technique for dielectric measurement of biological tissues: Challenges and common practices. *Diagnostics* **2018**, *8*, 40. [[CrossRef](#)]
29. Gabriel, S.; Lau, R.W.; Gabriel, C. The dielectric properties of biological tissues: II. Measurements in the frequency range 10 Hz to 20 GHz. *Phys. Med. Biol.* **1996**, *41*, 2251. [[CrossRef](#)]
30. Cole, K.S.; Cole, R.H. Dispersion and absorption in dielectrics I. Alternating current characteristics. *J. Chem. Phys.* **1941**, *9*, 341–351. [[CrossRef](#)]

31. Meaney, P.M.; Goodwin, D.; Golnabi, A.H.; Zhou, T.; Pallone, M.; Geimer, S.D.; Burke, G.; Paulsen, K.D. Clinical microwave tomographic imaging of the calcaneus: A first-in-human case study of two subjects. *IEEE Trans. Biomed. Eng.* **2012**, *59*, 3304–3313. [[CrossRef](#)]
32. Bjelogrić, M.; Fuchs, B.; Thiran, J.P.; Mosig, J.R.; Mattes, M. Experimental verification of optimal frequency range for microwave head imaging. In Proceedings of the 19th International Conference on Electromagnetics in Advanced Applications (ICEAA), Verona, Italy, 11–15 September 2017; pp. 1008–1011. [[CrossRef](#)]
33. Keysight Technologies. *Keysight 85070E Dielectric Probe Kit 200 MHz to 50 GHz*; Keysight Technologies: Santa Rosa, CA, USA, 2017.
34. Piladaeng, N.; Angkawisittpan, N.; Homwuttivong, S. Determination of relationship between dielectric properties, compressive strength, and age of concrete with rice husk ash using planar coaxial probe. *Meas. Sci. Rev.* **2016**, *16*, 14–20. [[CrossRef](#)]
35. Šarolić, A.; Matković, A. Dielectric permittivity measurement using open-ended coaxial probe—Modeling and simulation based on the simple capacitive-load model. *Sensors* **2022**, *22*, 6024. [[CrossRef](#)]
36. Dev, S.R.S.; Raghavan, G.S.V.; Garipey, Y. Dielectric properties of egg components and microwave heating for in-shell pasteurization of eggs. *J. Food Eng.* **2008**, *86*, 207–214. [[CrossRef](#)]
37. Feng, W.; Lin, C.P.; Deschamps, R.J.; Drnevich, V.P. Theoretical model of a multisection time domain reflectometry measurement system. *Water Resour. Res.* **1999**, *35*, 2321–2331. [[CrossRef](#)]
38. Hasgall, P.A.; Di Gennaro, F.; Baumgartner, C.; Neufeld, E.; Lloyd, B.; Gosselin, M.C.; Payne, D.; Kuster, N. *IT'IS Database for Thermal and Electromagnetic Parameters of Biological Tissues, Version 4.0.*; IT'IS Foundation: Zürich, Switzerland, 2018.
39. Gabriel, C. *Compilation of the Dielectric Properties of Body Tissues at RF and Microwave Frequencies*; Report N.AL/OE-TR-1996-0037; Occupational and Environmental Health Directorate, Radiofrequency Radiation Division, Brooks Air Force Base: San Antonio, TX, USA, 1996.
40. Joachimowicz, N.; Conessa, C.; Henriksson, T.; Duchêne, B. Breast phantoms for microwave imaging. *IEEE Antennas Wirel. Propag. Lett.* **2014**, *13*, 1333–1336. [[CrossRef](#)]

**Disclaimer/Publisher's Note:** The statements, opinions and data contained in all publications are solely those of the individual author(s) and contributor(s) and not of MDPI and/or the editor(s). MDPI and/or the editor(s) disclaim responsibility for any injury to people or property resulting from any ideas, methods, instructions or products referred to in the content.